Title
Microglial Activation in Mice Overexpressing Human Wildtype Alpha-Synuclein

Author
Lee, Soo Kyung

Publication Date
2012

Peer reviewed|Thesis/dissertation

UNIVERSITY OF CALIFORNIA

Los Angeles

Microglial Activation

In Mice Overexpressing Human Wildtype Alpha-Synuclein

A thesis submitted in partial satisfaction

of the requirements for the degree Master of Science

in Physiological Science

by

Soo Kyung Lee

2012

ABSTRACT OF THE THESIS

Microglial Activation

In Mice Overexpressing Human Wildtype Alpha-Synuclein

By

Soo Kyung Lee

Master of Science in Physiological Science

University of California, Los Angeles, 2012

Professor Mark Arthur Frye, Co-chair

Professor Marie-Françoise Chesselet, Co-chair

Parkinson's disease (PD) is a chronic and progressive neurodegenerative disorder characterized by a loss of nigrostriatal dopaminergic neurons. Although the etiology of PD is largely unknown, it is thought to arise from a combination of genetic and environmental factors. Alpha-synuclein, a protein involved in familial PD and a major constituent of the Lewy bodies found in sporadic PD, has recently been implicated as an initiator of microglial activation and neuroinflammatory processes in the pathogenesis of PD. The objective of this study was to determine if alpha-synuclein overexpression in the absence of overt neurodegeneration is sufficient to trigger microglial activation and the timeline of these inflammatory events. To test this hypothesis, I used the Thy1-aSyn mouse model, which overexpresses human wildtype alpha-synuclein under

the Thy-1 promoter. These mice demonstrate early and progressive sensorimotor anomalies in behavioral tests sensitive to nigrostriatal dysfunction and olfactory deficits, showing a loss of dopamine at 14 months of age. Previous studies by our group revealed that there was phenotypically specific microglial activation in the substantia nigra and striatum of Thy1-aSyn mice at 6 and 14 months of age, which was associated with exclusively increased TNF-α levels. This present thesis specifically examined neuroinflammation in Thy1-aSyn mice at 1 month of age to determine whether similar patterns of microglial activation are evident in earlier stages of development. By using Iba-1 immunohistochemistry, I found that there was a significant increase in microglial activation exclusively in the striatum of Thy1-aSyn mice compared to wildtype at 1 month of age. Microglial activation was accompanied by increased striatal TNF-α mRNA expression measured by quantitative RT-PCR. Tyrosine hydroxylase (TH) immunofluorescence confirmed that such changes in neuroinflammation occurred in the absence of dopaminergic terminal loss in the nigrostriatal pathway, and synaptophysin immunofluorescence evaluated the absence of synaptic loss in the striatum. Together, these data demonstrate that widespread overexpression of alpha-synuclein results in early microglial activation in the striatum that is associated with a distinct pro-inflammatory cytokine increase characterized by TNF-α production. Thus, the results of this study suggest that alpha-synuclein overexpression itself is capable of activating early inflammatory events that may be associated with PD pathology.

The thesis of Soo Kyung Lee is approved.

_____
Stephanie A. White

_____
Mark Arthur Frye, Committee Co-Chair

_____
Marie-Françoise Chesselet, Committee Co-Chair

University of California, Los Angeles

2012

DEDICATION

This thesis is dedicated to my family – my constant source of strength, hope and inspiration. Their unwavering support and unconditional love has allowed me to freely chase after my dreams and to see times of adversity as opportunities for growth. I also dedicate this thesis to Aram, for always believing in me when I did not. Above all, I thank JC, who breathes Life in me and always works for the good of those who love Him (Romans 8:28).

TABLE OF CONTENTS

LIST OF FIGURES

ACKNOWLEDGMENTS

This thesis would not have been possible without the guidance of my research mentor, Dr. Marie-Françoise Chesselet. I thank her for accepting me into her research group with open arms during one of the most difficult times in my graduate studies. I am truly privileged to be supported by such a distinguished scientist who continuously leads in the forefronts of scientific research with tireless academic dedication.

I would like to express my gratitude to my committee members, Dr. Stephanie White and Dr. Mark Frye, for their patience and support throughout this work. I thank Dr. White for her constant kindness and availability, and for sharing the use of her lab's cryostat- this thesis literally would not have come to fruition without her generosity. I thank Dr. Frye for challenging me time and time again to think like a real scientist and for proving through his own contagious passion that a life dedicated to science is invaluable.

My deepest thanks go to the members of the Chesselet lab who provided me with insightful critiques along with technical assistance that familiarized me to the lab. I give special thanks to Zachary Burkett from the White lab for allowing me to use their lab's cryostat and for his moral support throughout my graduate studies. I also thank Matt Uy and Dr. Alan Garfinkel for their help with the bootstrapping method and MATLAB codes for statistical analyses, and Hiroko Nobuta from the Waschek lab for allowing me to use their ELISA plate reader. Without their collaboration, this thesis would not be possible.

My experiences in graduate school would not nearly have been as memorable without the genuine care and intellectual stimulation from my beloved classmates and the faculty of the Physiological Science department. I must also acknowledge Michael Carr and the UCLA Graduate Division for guiding me through this filing process and for providing me with financial support in the form of a university fellowship and teaching appointments.

Finally, I would like to express my deepest gratitude to my direct supervisor, Dr. Melanie Watson. I am deeply indebted to Mel for her endless patience and direction throughout this project. She believed in me when I probably did not give her much reason to, and she continues to inspire me through her excitement and passion for science. I also want to personally thank her for directing me toward the path of dentistry. It has been an incredible honor and joy to have worked under her encouragement and guidance for the past two years.

Introduction

Parkinson's disease (PD) is a chronic and progressive neurodegenerative disorder affecting 500,000 individuals in the United States alone, with about 50,000 new cases being reported each year (National Institute of Neurological Diseases and Stroke). Age is the main risk factor of PD, affecting 1% of the population over the age of 65. PD was first described in 1817 by the English physician, James Parkinson. In his "An Essay on the Shaking Palsy," Parkinson illustrated the "shaking palsy" as "involuntary tremulous motion, with lessened muscular power, in parts not in action." PD is the most common movement disorder and is also the second most common neurodegenerative disease after Alzheimer's disease (AD). Clinically, the defining motor symptoms of PD are collectively referred as parkinsonism, which includes resting tremor, rigidity, postural instability, slowness in movement (bradykinesia) and difficulty in initiating movements (akinesia) (Lew et al. 2007, Jankovic et al. 2008, Davie et al. 2008). PD is also characterized by non-motor symptoms including anosmia, sleep disorders, gastrointestinal dysfunction, mood disorders, cognitive impairment, orthostatic hypotension, vocal deficits and swallowing disorders, where these non-motor symptoms can even precede parkinsonism (Chaudhuri et al. 2006, Ziemssen et al. 2007, Lew 2007, Sapir et al. 2008, Chaudhuri et al. 2009).

The classical pathophysiology of PD is viewed as the loss of dopaminergic neurons in the substantia nigra pars compacta (SNpc) of the basal ganglia. Post-mortem studies revealed that there was a specific depletion of melanin-containing dopaminergic neurons in the SNpc of PD patients compared to normal individuals (Braak et al. 2004). Neurons of the nigrostriatal pathway normally modulate motor commands by activating dopaminergic synapses with medium

spiny neurons of the striatum (Surmeier et al. 2007). In the direct pathway, dopamine released from the nigrostriatal neurons binds to D1 receptors in the striatum, causing GABAergic striatal neurons to inhibit GABAergic neurons in the globus pallidus internus (GPi). These inhibited GPi neurons then allow the disinhibition of thalamic neurons, exciting the premotor cortex to initiate motor commands. In the indirect pathway, dopamine from nigrostriatal neurons binds to D2 receptors in the striatum, inhibiting GABAergic striatal neurons projecting to GABAergic neurons in the globus pallidus externus (GPe). These disinhibited GPe neurons inhibit excitatory glutamatergic neurons in the subthalamic nucleus (STN), ultimately decreasing inhibitory GPi output to the thalamus and allowing for activation of the motor cortex. Therefore, dopamine released from SNpc neurons normally activates the direct pathway and restrains the indirect pathway, which normally acts as a "brake" to the direct pathway facilitatory effects. Therefore, dopamine facilitates voluntary movements by two complementary mechanisms. In contrast, disruption of dopamine to the striatum causes an abnormal inhibition of the direct pathway and excitation of the indirect pathway. Dysfunction in the nigrostriatal pathways results in the overall inability to initiate intended movements leading to the characteristic akinesia associated with PD (Lew 2007, Jankovic 2008, Davie 2008).

Another classical hallmark of PD is the presence of proteinaceous inclusions referred to as Lewy bodies in various regions of the central nervous system. Post-mortem studies observed that these insoluble aggregates first form in the medulla oblongata and olfactory bulb, progressing into areas of the midbrain and basal forebrain, including the substantia nigra. At this stage, the disease manifests itself in the full range of characteristic PD-associated clinical symptoms in living humans. The inclusion bodies finally reach the cerebral cortex during the end stages of

PD, eventually leading to severe cognitive deficits (Braak et al. 2003, Braak et al. 2004). It is particularly noteworthy that the presence of Lewy bodies is thought to precede the neurodegeneration involved in PD. Moreover, there have been implications that Lewy bodies affect neuronal circuits in the peripheral autonomic nervous system that control physiological functions in areas including the esophagus, stomach, colon, heart, bladder and skin (Lew 2007, Djaldetti et al. 2009). Such findings can explain the high prevalence of non-motor symptoms in PD patients. There is mounting evidence that dopaminergic cell loss in the nigrostriatal pathway is associated with the accumulation of Lewy bodies in PD, but the cause of these insoluble protein deposits still requires investigation.

Although the etiology of PD is still largely unknown, most PD cases are hypothesized to occur through both genetic and environmental factors. In fact, it is widely accepted that PD is a complex disorder that is most likely influenced by the interaction between genetic makeup and environmental influences, in which different pathogenic pathways and cellular mechanisms can lead to PD (Ross et al. 2007, Horowitz et al. 2010, Gao et al. 2011). Familial PD is believed to make up about 10% of all diagnosed cases. Mutations in six genes (SNCA, LRRK2, PRKN, DJ1, PINK1 and ATP13A2) have conclusively been found to cause familial PD. Mechanisms by which genetic mutations cause PD are not well known, but previous findings show that these genes are related to molecular abnormalities ranging from protein aggregation, defective ubiquitin-mediated protein degradation, mitochondrial dysfunction and oxidative damage (Bekris et al. 2010). Even though many cases of familial PD demonstrate pathologies and clinical manifestations that are not associated with sporadic PD, studying the genes responsible for familial PD can provide valuable insight into the pathological processes of sporadic PD. The

same genes and pathways altered in familial PD may also be modified by environmental influences that are associated with sporadic PD, such as pesticides, industrial toxins, brain trauma and inflammation (Chesselet et al. 2011, Gao et al. 2011). Therefore, creating genetic models of familial PD in combination with known environmental manipulations have provided and will continue to provide valuable information on the etiology and pathogenesis of sporadic PD.

Alpha-synuclein is a protein involved in familial PD that is considered to be involved in the pathogenesis of sporadic PD. The SNCA gene encodes for the soluble, 140 amino acid alpha-synuclein protein that is expressed ubiquitously expressed throughout the brain (Maroteaux et al. 1991). Previous research shows that natively unfolded alpha-synuclein takes on an alpha-helical structure when bound to membranes or vesicles (Davidson et al. 1998). Because alpha-synuclein is concentrated at presynaptic nerve terminals in close proximity to synaptic vesicles, there has been ongoing research suggesting that the protein plays a role in neurotransmitter release and synaptic plasticity (Clayton et al. 1999, Lykkebo et al. 2002, Watson et al. 2009, Stefanis 2012). Abnormally aggregated alpha-synuclein is a major constituent of Lewy bodies, in which the protein accumulates in a progressive and sequential manner as confirmed by post-mortem studies of PD (Braak et al. 2004). Point mutations, duplications and triplications in the SNCA gene have been identified to cause rare familial forms of PD (Polymeropoulos et al. 1997, Kruger et al. 1998, Singleton et al. 2003, Ibanez et al. 2004). The various genetic mutations in the SNCA gene result in greater expression of the normal protein in PD patients than in normal individuals. Moreover, modifications of alpha-synuclein including aggregation, nitration and oxidation have

been shown to be toxic to dopaminergic neurons (Gao et al. 2008, Reynolds et al. 2008, Lee et al. 2010).

Increasing evidence has linked alterations in neuroinflammation to the neurotoxicity of alpha-synuclein in the nigrostriatal pathway. Post-mortem analyses indicated a widespread but mild inflammatory response throughout the central nervous system of PD patients (Banati et al. 1998, Hunot et al. 2003, Hirsch et al. 2003, Imamura et al. 2003). Increased numbers of activated microglia were observed in the substantia nigra of PD patients (McGeer et al. 1988, Kim et al. 2006). Additionally, pathological studies demonstrated a relationship between activated microglia and alpha-synuclein deposition in the substantia nigra of PD patients (Croisier et al. 2005). Furthermore, increased levels of pro-inflammatory cytokines were found in the cerebrospinal fluid of PD patients along with the identification of $CD4^+$ and $CD8^+$ T lymphocytes in the substantia nigra of PD patients (Nagatsu et al. 2000, Brochard et al. 2009). Activation of microglia, increased levels of pro-inflammatory cytokines and the presence of $CD4^+$ and $CD8^+$ T lymphocytes have also been confirmed in the substantia nigra and the striatum of 1-methyl-4-phenyl-1,2,3,6-tetrahydropyridine (MPTP)-treated parkinsonian mice (Francis et al. 1995, Czlonkowska et al. 1996, Nagatsu et al. 2005, Su et al. 2008). Emerging research notes that the accumulation of wildtype, mutated and pathological species of alpha-synuclein actually induce microglial activation *in vitro* (Zhang et al. 2005, Klegeris et al. 2006, Zhang et al. 2007, Reynolds et al. 2008, Klegeris et al. 2008, Su et al. 2009, Sanchez-Guajardo et al. 2010). Together, these data suggest the significant role of alpha-synuclein-induced inflammation in the pathogenesis of PD.

The aim of this thesis was to determine if alpha-synuclein overexpression, in the absence of overt neurodegeneration, is sufficient to trigger microglial activation in the nigrostriatal pathway of mice. To test this hypothesis, I utilized the Thy1-aSyn mouse model, which overexpresses human wildtype alpha-synuclein under the Thy-1 promoter (Rockenstein et al. 2002). These mice display widespread overexpression and accumulation of alpha-synuclein throughout the brain, with the formation of alpha-synuclein aggregates in the olfactory bulbs, substantia nigra and locus coeruleus (Chesselet et al. 2012). Furthermore, these mice have early and progressive sensorimotor anomalies in behavioral tests sensitive to nigrostriatal dysfunction and olfactory deficits (Fleming et al. 2004, Fernagut et al. 2007, Fleming et al. 2008) and a loss of dopamine at 14 months of age (Lam et al. 2011). Previous studies by our group revealed that there was microglial activation in the substantia nigra and striatum of Thy1-aSyn mice at 6 and 14 months, which was associated with exclusively increased levels of the pro-inflammatory cytokine tumor necrosis factor-alpha (TNF-α). The adaptive immune response in these mice was upregulated at 22 months of age through the increase of $CD8^+$ T lymphocytes, with no apparent neurodegeneration of the nigrostriatal pathway until 14 months of age (Lam et al. 2011). To determine whether such phenotypically distinct patterns of microglial activation are evident in earlier stages of development, this present thesis sought to examine differences in neuroinflammation between Thy1-aSyn mice and wildtype littermates at 1 month of age. Investigating the relationship between alpha-synuclein overexpression and microglial activation in the nigrostriatal pathway would therefore increase our understanding of the role and subsequent effects of inflammation in the pathology of PD.

Materials and Methods

Animals

Groups of 1-month-old wildtype (WT) and transgenic mice overexpressing human wildtype α-synuclein under the Thy-1 promoter (Thy1-aSyn) were used in this study. Thy1-aSyn mice were crossed into a mixed C57BL/6-DBA/2 background (Rockenstein et al. 2002), and only male mice were used to avoid inconsistencies due to random inactivation of the X chromosomes (that harbors the transgene) in females. Mice weight ranged from 20 to 30 grams. Animals were maintained on a reverse light/dark cycle, and food and water were available *ad libitum*. Animal care was conducted in accordance with the United States Public Health Service Guide for the Care and Use of Laboratory Animals, and procedures were approved by the Institutional Animal Care and Use Committee at the University of California, Los Angeles.

Dissections and preparation of tissue

The WT and Thy1-aSyn mice were divided into two groups. The first group (n=6) was anesthetized with pentobarbital (100 mg/kg, i.p.) and perfused through the left ventricle of the heart with 0.1M PBS followed by 4% paraformaldehyde (PFA) in PBS. Brains were quickly removed, postfixed in 4% PFA, cryoprotected in 30% sucrose in 0.1M PBS, frozen with powdered dry ice, and stored at −80°C. Free-floating coronal sections (40 μm thick) were cut using a cryostat and stored in cryoprotectant for immunohistochemical analysis. The second group (n=6-8) was anesthetized with pentobarbital (100 mg/kg, i.p.). Mice were then perfused through the left ventricle of the heart with 0.1M PBS. Brains were quickly removed, and nigral, striatal and cortical tissue blocks were extracted and fresh frozen in powdered dry ice for mRNA and protein analysis.

Measurement of inflammation using Iba-1 immunohistochemistry

For assessment of microglial activation, ionized calcium binding adaptor molecule 1 (Iba-1) was measured by 3,3'-diaminobenzidine tetrachloride (DAB) immunohistochemistry. Sections of the substantia nigra and medial striatum from PFA-perfused WT and Thy1-aSyn mice were arbitrarily selected, washed in 0.1M PBS, and incubated in a blocking solution containing 1% H_2O_2 in PBS for 30 minutes at room temperature to inhibit endogenous peroxidase activity. The sections were washed in 0.1M PBS, and blocked in 0.1M PBS containing 10% normal goat serum (NGS) and 0.5% Triton X for 2 hours at room temperature. The sections were then incubated overnight at 4°C in rabbit anti-Iba-1 polyclonal antibody (1:500, Wako 019-19741, Richmond, VA) in 5% NGS and 0.5% Triton X in 0.1M PBS. After washing with 0.1M PBS, sections were incubated with a biotinylated goat anti-rabbit igG antibody (1:200, Vector Labs BA-1000, Burlingame, CA) in 0.1M PBS with 5% NGS for 2 hours at room temperature. The avidin-biotin complex method was used to detect the secondary antibody (Vectastain Elite ABC kit, Vector Labs PK-6100, Burlingame, CA) for 1 hour and washed in 50mM Tris-HCl. The reaction product was visualized by incubation in 50mM Tris-HCl (pH 7.4) containing 0.05% DAB (Sigma-Aldrich D4418, USA) and 0.01% H_2O_2. After the reaction, sections were dehydrated in graded ethanol steps, cleared with xylene and mounted onto gelatin-coated glass slides. Control sections were incubated with no primary antibody to verify specificity of primary antibody binding.

Quantification of microglial activation

Microglial activation was assessed by an investigator blind to genotype in sections of striatum, and SN from 1 month old WT and Thy1-aSyn mice stained with IBA-1 (as described above). IBA-1 is expressed by both resting and activated microglia (Rappold et al., 2006) and morphologically distinct classes of IBA-1-positive cells can be distinguished based on cell body diameter. Microglia with cell body diameters less than 5 μm have a resting morphology characterized by multiple ramified processes, hyper-ramified microglia/partially activated microglia had mean cell body diameters of 5-6 μm, and fully activated amoeboid microglia had mean cell body diameters of 7-14 μm have an activated morphology characterized by ameboid cell bodies with few, short processes (Batchelor et al., 1999). Accordingly, microglial activation was quantified by measuring the diameter of IBA-1-positive cells. Analysis was done on a Leica DM-LB microscope with a Ludl XYZ motorized stage and z-axis microcator (MT12, Heidenheim, Traunreut, Germany) using StereoInvestigator software (MicroBrightField, Colchester, VT). StereoInvestigator software was used for ease of counting and to enable measurements of microglial diameters. The sampling protocol was systematic and microglial measurements were made in every 5th counting frame. A contour was drawn to delineate the striatum, SN, cerebral cortex and cerebellum under the 5x objective lens to ensure anatomical accuracy. Following delineation, the diameters of microglial cell bodies were measured in the first counting frame (100μm) and then in every fifth counting frame at 40x magnification. This sampling frequency was chosen in order to count approximately 30-50 IBA-1+ cells in each side of the SN. The first counting frame was always positioned in the upper left corner of the contour and systematically moved from left to right and from top to bottom. Microglia were counted and quantified in every 5th counting frame of the delineated contour regions. We determined the frequency of IBA-1+ microglia cells with cell diameters ranging from 1μm to 14μm. The

number of cells with each diameter was normalized to the total number counted in each section and expressed as a percentage of total microglial cells.

mRNA extraction

mRNA was extracted from fresh frozen nigral, striatal and cortical tissue from WT and Thy1-aSyn mice (n=7 mice/group) that were perfused through the left ventricle with 0.1M PBS. For all samples, 30 mg of microdissected tissue were thawed on ice and cell lysis mastermix (353.5 µl, Nucleospin RNA II, Clontech Laboratories 740955.50, Mountain View, CA) containing β-mercaptoethanol was added to each Eppendorf tube. The samples were homogenized in the cell lysis mastermix for extraction of RNA. To remove any insoluble tissue and reduce viscosity, the homogenized lysate was added to a NucleoSpin filter unit placed in an Eppendorf collecting tube and centrifuged at 11,000 X g for 1 minute. The NucleoSpin Filter unit was discarded and 70% ethanol (350 µl, Sigma-Aldrich, USA) was added to the lysate. The ethanol and lysate were mixed to improve RNA binding to the NucleoSpin RNA II columns, which the lysates were loaded onto. The new column was placed in a collecting tube, and these were centrifuged at 8,000 X g for 30 seconds. The column was placed in a new collecting tube and membrane-desalting buffer (350 µl) was added to allow the subsequent RNase-free DNases to digest the samples more effectively. The sample was centrifuged at 11,000 X g for 1 minute to dry the membrane. DNA was digested by adding DNase reaction (95 µl) to the column and incubated at room temperature for 15 minutes. The silica membrane of the NucleoSpin RNA II column was washed with RA2 buffer (200 µl) to inactivate the DNases, centrifuged at 8,000 X g for 30 seconds to dry, and placed in a new collecting tube. The silica membrane was washed with RA3 buffer (600 µl), centrifuged at 8,000 X g for 30 seconds to dry, and added to a new collecting

tube. The silica membrane was washed with RA3 buffer (250 μl), centrifuged at 11,000 X g for 2 minutes to completely dry the membrane, and placed into labeled nuclease-free 1.5 ml Eppendorf tubes. Pure RNA was finally eluted from the column by adding RNase-free H_2O (40 μl) and centrifuging at 11,000 g for 1 minute. RNA concentrations were quantified using a Nanodrop spectrophotometer (ND-1000 V3.5, Nanodrop Technologies, Inc., USA).

Reverse transcription for cDNA synthesis

Total RNA concentration was equalized to 200 μg/ml before cDNA synthesis using a High Capacity cDNA Reverse Transcription Kit (Applied Biosystems 4368814, Foster City, CA). RNA (20 μl) was added to fresh tubes containing nuclease-free H_2O (8.4 μl), which will subsequently make up a final volume of 20 μl of mastermix per every 20 μl of RNA sample. A mastermix was prepared on ice containing 10x reverse transcription buffer (4 μl), 25x dNTPs (1.6 μl), 10x random primers (4 μl) and multiscribe reverse transcriptase (2 μl, 50 μg/μl). The mastermix (11.6 μl per sample) was added to the RNA and nuclease-free H2O, for a 1:1 ratio of nuclease-free H2O and mastermix to RNA. Tubes were incubated for 10 minutes at 25°C followed by 2 hours at 37°C on a thermocycler (Mastercycler gradient thermocycler, Eppendorf, Hauppauge, NY).

cDNA amplification by quantitative real-time PCR

Real-time PCR primers were delivered as "Taqman® Gene Expression Assays" containing forward and reverse primers, and a FAM-labeled MGB Taqman® probe for each gene (Applied Biosystems, Foster City, CA). Primers used were as follows: CD11b (Taqman® Gene Expression Assay No. Mm00445235_m1), F4/80 (Mm00444543_m1), IL-1β (Mm00434228_m1), IL-6

(Mm00446191_m1), TNF-α (Mm0043258_m1), TGF-β (Mm0041895_m1), MCP-1 (Mm00441242_m1), β-actin (Mm00607939_s1), HPRT (Mm01545399_m1), and ATP5B (Mm01160396_g1). A 2:9 dilution of cDNA was prepared (1 μl cDNA in 3.5 μl RNA-free H_2O) and added in triplicates to each well of a 384-well plate. 0.5 μl of the respective primer and 5 μl of Taqman® Gene Expression mastermix (Applied Biosystems 4369016, Foster City, CA) were added to each well, resulting in a total reaction volume of 10 μl per well. Plates were centrifuged at 2000 g for 1 minute in preparation for the PCR reaction. Quantitative real-time PCR was performed using the Applied Biosystems 7300 Real-time PCR System. cDNA was mixed with SYBR Green PCR Master Mix (Invitrogen 11760-100, Carlsbad, CA), supplied in a 2x concentration and containing SYBR Green I Dye, AmpliTaq Gold DNA Polymerase, dNTPs with dUTP, Passive Reference and optimized buffer component, and the respective gene assay. Direct detection of PCR product was monitored by measuring the increase in fluorescence caused by the binding of SYBR Green dye to double-stranded DNA. Mouse β-actin, HPRT and ATP5B were used as endogenous control references, and expression was conducted using a gene expression assay containing forward and reverse primers and a VIC-labeled MGB Taqman probe (#4352340E; Applied Biosystems, Foster City, CA). Forty to sixty cycles were run as follows: 10 minutes at 95 °C, and for each cycle, 15 seconds at 95 °C for denaturation and 1 minute at 60 °C for elongation of the PCR product. A dissociation curve that plotted changes in fluorescence against temperature was generated through computer software to check for nonspecific product formation.

Q-PCR quantification

The expression of each target gene was determined using the efficiency-corrected comparative CT method. The geNorm algorithm (geNorm, version 3.5, PrimerDesign Ltd., http://medgen.ugent.be/~jvdesomp/genorm) was used to determine the most stable housekeeping gene out of the three reference genes, and a gene expression normalization factor was calculated for each sample based on the geometric mean of three reference genes. Gene expression was calculated using the normalization factor and analysis was performed using the $2^{-\Delta\Delta CT}$ method.

Analysis of TNF-α concentrations

TNF-α protein concentrations in the striatum were analyzed by ELISA using the Mouse TNF (Mono/Mono) ELISA Set (BD Biosciences 555268, San Diego, CA). Sections of the left striatum were homogenized in 500 µl of 0.2% Krebs Calcium solution. Samples were centrifuged for 15 minutes at 14,000 X g in 4°C, and the supernatants were extracted into new Eppendorf tubes. To measure the protein concentrations of the samples, a protein assay was prepared using the Bio-Rad Quick Start Bradford 1x Dye Reagent (Bio-Rad 500-0205, Hercules, CA) and Bio-Rad Quick Start Bovine Serum Albumin (BSA) Standard Set (Bio-Rad 500-0207, Hercules, CA). 20 µl of samples diluted 1 in 10 fold with nuclease-free water, and 8 BSA standards with concentrations of 0, 0.125, 0.25, 0.5, 0.75, 1, 1.5 and 2.0 mg/ml, were added to 980 µl of the Bradford 1x Dye Reagent in plastic cuvets. After incubating at room temperature for 5 minutes, absorbance was measured at 595 nm using a spectrophotometer. A standard curve was generated based on the concentrations and absorbances of the BSA standards, and protein concentrations of the samples were calculated and equalized to 1.5 mg/ml. A 96-well ELISA plate was coated with rat anti-mouse TNF-α capture antibody (50 µl per well; 0.8 µg/ml) overnight at 4°C. The plate was washed three times with wash buffer (PBS

with 0.05% Tween-20) and blocked with assay diluent (200 µl per well; PBS containing 10% FBS) for 1 hour at room temperature. After washing three times with wash buffer, triplicate samples and TNF-α standards (50 µl per well; 0-2000pg/ml recombinant mouse TNF-α) were added to appropriate wells in a randomized fashion and incubated for 2 hours at room temperature. Samples were washed five times with wash buffer and incubated for 1 hour at room temperature in the presence of the detection antibody (50 µl per well; 150 ng/ml biotinylated rat anti-mouse TNF-α) and the detection reagent (HRP-conjugated streptavidin; 1:250 dilution in diluted detection antibody). Samples were washed seven times with wash buffer and substrate solution (50 µl per well; 1:1 mixture of H_2O_2 and tetramethylbenzidine) was added. Samples were incubated in the dark for 20 to 30 minutes at room temperature and the reaction was stopped using 1M H_2SO_4 (25 µl per well). Absorbance of the plate was read at 450 nm. TNF-α concentrations were estimated from the appropriate standard curve and expressed as pg/mg of protein.

Measurement of circulating T cells by flow cytometry

Blood (500 µl) was collected by retroorbital blood letting and cardiac puncture from 1 month old WT and Thy1-aSyn mice and placed into tubes containing Heparin (50 µl). Red blood cell lysis buffer (9 ml) was added to blood and samples were incubated on ice for 7 minutes. 0.1M PBS was added to inactivate the lysis buffer and samples were centrifuged at 1800 rpm for 7 minutes to retrieve the pellet. The supernatant was removed and the pellet was reconstituted in 1 ml of RPMI. The cells were counted using a hemocytometer and equalized to 1 million cells. Cells were centrifuged at 1800 rpm for 7 minutes in 1% BSA in 0.1M PBS at 4°C to wash the cells. The supernatant was removed and cells were incubated with a mixture of PeCy7 rat anti-

mouse CD4 (BD Biosciences 552775, San Diego, CA) and APC rat anti-mouse CD8 (BD Biosciences 553035, San Diego, CA) antibodies diluted in 1% BSA in 0.1M PBS for 30 minutes at 4°C in the dark. Negative controls were incubated with 1% BSA in 0.1M PBS and single-colored cells were incubated with PeCy7 rat anti-mouse CD4 or anti-mouse APC rat anti-mouse CD8 antibodies. Cells were centrifuged at 1800 rpm for 7 minutes in 1% BSA in 0.1M PBS at 4°C to wash the cells. Supernatants were removed and cells were reconstituted in 300 μl 1% BSA in 0.1M PBS before reading on the flow cytometry machine.

Assessment of striatal neuropathology

For assessment of striatal neuropathology, rostral, medial and caudal sections of the striatum from WT and Thy1-aSyn mice were stained for tyrosine hydroxylase (TH), and synaptophysin. Sections washed in 0.1M PBS and blocked in 5% normal goat serum (NGS) and 0.5% Triton X in 0.1M PBS for 1 hour at room temperature. Sections were then incubated overnight at 4°C in 2% NGS in 0.1M PBS with the respective primary antibody: rabbit anti-mouse TH (1:200, Millipore AB152, Hayward, CA) or anti-mouse synaptophysin (1:200, Millipore MAB5258, Hayward, CA). After washing in 0.1M PBS, the sections were incubated for 1 hour in the dark in 0.1M PBS with 2% NGS, 0.5% Triton X, and the respective secondary antibody: goat anti-rabbit Cy3 (1:400, Millipore AP187C, Hayward, CA) for TH immunofluorescence or anti-mouse Cy5 (1:500, Millipore AP187C, Hayward, CA) for synaptophysin immunofluorescence. Sections were washed in 0.1M PBS and mounted onto uncoated glass slides. Sections were processed using the microarray tissue scanner and fluorescence intensity was analyzed using ImageJ software (ImageJ Software, version 1.43, National Institute of Health; http://rsbweb.nih.gov/ij/).

Statistical analysis

The frequency distribution of microglial activation was analyzed using the bootstrapping method (Efron and Tibshirani, 1991) coded through the MATLAB (The MathWorks Inc., Natick, MA) program. The bootstrapping method is an appropriate method of analysis for this frequency of distribution because it requires no special probability assumptions regarding the shape and size of the populations being sampled from, and thus is fitting to use for populations that are not normally distributed or cannot be determined as having a normal distribution due to small sample size and the presence of outliers. I first calculated the group mean microglial diameters of the WT mice. The frequency of distribution of the WT means was my test statistic, M. I resampled this test statistic by using a box model for simulation, and generated M values. This resampling process was repeated 1000 times, and the M values of the WT microglial diameters were plotted onto a histogram. The 2.5% and 97.5% cut-off values of the M values were calculated to find the 95% confidence interval (CI). The 95% CI was also calculated for the actual group mean microglial diameters of Thy1-aSyn mice. These 95% CI bands were compared to assess whether the actual mean microglial diameters of Thy1-aSyn mice were statistically significant at the $p < 0.05$ level, independent of assumptions about probability distributions. Specifically, any 95% CI band of Thy1-aSyn data that does not land within the 95% CI bands created from the resampled WT means is considered to be statistically significant to the $p < 0.05$ level. Microglial activation and cytokine gene expressions, and TNF-α protein concentration were analyzed by two-tailed, unpaired Student's t-tests. Significance for percentages of T cells in the blood was analyzed by non-parametric Mann-Whitney tests. I also analyzed striatal TH and synaptophysin expressions by one-way ANOVA, followed by a

Fisher's LSD post-hoc test. All statistical analyses are represented as mean ± standard error of the mean, and were conducted with GraphPad Prism 4 software (GraphPad Software, La Jolla, CA). The level of significance was set at $p < 0.05$.

Results

Overexpression of human wildtype alpha-synuclein in Thy-1- a-Syn mice leads to microglial activation in the striatum at one month of age

Previous studies by our group demonstrated that widespread alpha-synuclein overexpression in Thy1-aSyn mice resulted in microglial activation at 6 and 14 months of age that was not associated with dopaminergic cell death in the nigrostriatal pathway (Watson et al. 2012). To determine whether such patterns of neuroinflammation could be detected in Thy1-aSyn mice at an earlier time point, this study quantitatively evaluated Iba-1 immunohistochemistry in the substantia nigra and striatum of Thy1-aSyn and WT littermates at 1 month of age. Microglia phenotypes were determined based on cell body diameters, in which resting microglia had smaller cell body diameters (Figure 1A, black arrow) and activated microglia had bigger cell body diameters (Figure 1B, white arrow). No significant differences in Iba-1^+ microglia counts in the substantia nigra were observed between groups (n = 4 per group) (Figures 1C, 1D). Meanwhile, bootstrapping revealed a significant increase in the number of activated Iba-1^+ microglia in the striatum of Thy1-aSyn mice compared to WT (n=3 per group), with no significant differences in total Iba-1^+ microglia counts between groups (Figure 2). To further evaluate microglial activation in the substantia nigra and striatum of Thy1-aSyn mice, we measured the mRNA expression of microglia marker CD11b using quantitative RT-PCR. Since CD11b is constitutively expressed by many leukocytes including microglia, this microglial marker was used to assess whether there were differences in microglia numbers in the substantia nigra and striatum between Thy1-aSyn mice and WT littermates. Student's t-test revealed no significant differences in CD11b mRNA expression in either the substantia nigra (Thy1-aSyn: 0.5383 ± 0.0583, WT: 0.4393 ± 0.0388, p = 0.2002, n = 6-7 per group) or the striatum (Thy1-

aSyn: 0.9352 ± 0.0569, WT: 0.9499 ± 0.1608, p = 0.9328, n = 7 per group) between groups. These results indicate that there is specific localized microglial activation in the striatum of Thy1-aSyn mice that is not found in the substantia nigra at this time point.

The cytokine pathway induced by human wildtype alpha-synuclein is restricted to TNF-α

To determine the functionality of activated microglia in of Thy1-aSyn mice at one month of age, I examined pro-inflammatory (TNF-α, IL-6, IL-1β) and anti-inflammatory (TGF-β) cytokine mRNA expressions in nigrostriatal regions of the brain by quantitative RT-PCR. Student's t-test revealed that TNF-α mRNA expression was significantly increased in the striatum of Thy1-aSyn mice compared to WT at one month of age (Thy1-aSyn: 0.8092 ± 0.0608, WT: 0.5979 ± 0.0643, p = 0.0342, n = 7 per group) (Figure 3A). No other pro-inflammatory (IL-6, IL-1β) or anti-inflammatory (TGF-β) cytokine mRNA levels were found to be significantly different in the striatum between groups (IL-6: Thy1-aSyn 0.7708 ± 0.0559 vs. WT 0.6682 ± 0.0406, p = 0.1634; IL-1β: Thy1-aSyn 0.6313 ± 0.0677 vs. WT 0.6693 ± 0.0906, p = 0.7424; TGF-β: Thy1-aSyn 0.7802 ± 0.0421 vs. WT 0.7840 ± 0.0293, p = 0.9413; n = 7 per group) (Figure 3A). ELISA was used to assess whether the increase in TNF-α mRNA expression translated into increased protein concentration in the striatum of Thy1-aSyn mice. Student's t-test revealed no significant differences in TNF-α protein concentration between groups (Thy1-aSyn: 22.38 ± 8.60 pg/mg, WT: 10.00 ± 2.850 pg/mg, p = 0.2092, n = 5 per group), but there was a trend toward increased TNF-α protein levels in the striatum of Thy1-aSyn mice compared to WT (Figure 4). None of the classic pro-inflammatory and anti-inflammatory cytokines were significantly altered in the substantia nigra (TNF-α: Thy1-aSyn 0.6344 ± 0.0826 vs. WT 0.4706 ± 0.0750, p = 0.1678; IL-6: Thy1-aSyn 0.7236 ± 0.0622 vs. WT 0.7467 ± 0.1187, p = 0.8663; IL-1β: Thy1-aSyn 0.6759 ±

0.1177 vs. WT 0.6522 ± 0.0625, p = 0.8690; TGF-β: Thy1-aSyn 0.6320 ± 0.0942 vs. WT 0.6106 ± 0.0591, p = 0.8508; n = 6-7 per group) (Figure 3B) or in the cortex (data not shown) compared to WT at one month of age. Together, these results suggest that microglial activation in the striatum is associated with a distinct pro-inflammatory cytokine network through the production of TNF-α.

No significant changes in the adaptive immune response occur in Thy1-aSyn mice at one month of age

The above data suggest that the overexpression of human alpha-synuclein results in specific microglial activation that triggers the pro-inflammatory TNF-α pathway in Thy1-aSyn mice. To examine whether this innate immune response causes alterations in the adaptive immune response in Thy1-aSyn mice at one month of age, $CD4^+$ and $CD8^+$ T lymphocytes concentrations were assessed in the blood using flow cytometry. A Mann-Whitney test revealed that there was no significant difference in levels of $CD4^+$ and $CD8^+$ T lymphocytes in the blood of Thy1-aSyn mice compared to WT littermates ($CD4^+$: Thy1-aSyn 21.33 ± 4.88 vs. WT 27.37 ± 1.56, p = 0.7000; $CD8^+$: Thy1-aSyn 10.97 ± 3.26 vs. WT 13.73 ± 1.64, p = 0.7000; n = 3 mice per group) (Figure 5). Based on this data, there is no clear indication that microglial activation directly causes alterations in the adaptive immune response of Thy1-aSyn mice.

Striatal neuropathology is not present in Thy1-aSyn mice at one month of age

Considering that this specific inflammatory microglial phenotype is present only in the striatum of Thy1-aSyn mice at one month of age, this study investigated whether there was striatal neuropathology at this time point that was causing specific microglia activation. Tyrosine

hydroxylase (TH) and synaptophysin immunofluorescence was used in rostral, medial and caudal sections of the striatum to determine any loss of dopaminergic axon terminals and/or loss of synapses at this early time point. TH immunofluorescence was used as an indirect measure of dopaminergic terminals originating from neurons from the substantia nigra pars compacta to the striatum. One-way ANOVA revealed no significant difference in TH immunofluorescence in rostral, medial and caudal sections of the striatum between groups ($F(5,30) = 0.6917$, $p = 0.6336$, $n = 6$ mice per group) (Figure 6A, 6C). One-way ANOVA also indicated no significant difference in synaptophysin immunofluorescence in rostral, medial and caudal striatal sections between groups ($F(5,27) = 0.3083$, $p = 0.9036$, $n = 6$ mice per group) (Figure 6B, 6D). From these data, it is deduced that there is no striatal neuropathology in Thy1-aSyn mice at one month of age. These results illustrate that distinct microglial activation in the striatum occurs at a time when there is no dopaminergic cell death in this mice that have widespread overexpression of human wildtype alpha-synuclein.

Discussion

In this present thesis, I sought to determine whether overexpression of human wildtype alpha-synuclein could induce similar patterns of microglial activation in the nigrostriatal pathway of Thy1-aSyn mice as previously reported at an earlier stage of development. Immunohistochemical methods revealed that there was a significant increase in the number of activated amoeboid microglia in the striatum of Thy1-aSyn mice at 1 one of age. Such microglial activation localized in the striatum was found to be associated with an increase in TNF-α mRNA expression at this time point. Although this present thesis presented that Thy1-aSyn mice did not demonstrate an upregulation in TNF-α protein concentrations at one month of age, subsequent analyses from our group has revealed a significant increase in TNF-α protein concentrations at this age (Watson et al. 2012). These early neuroinflammatory changes occur in the absence of striatal neuropathology as suggested by TH and synaptophysin immunofluorescence. However, subtle changes could have been missed in this study that used frozen sections, a method less sensitive to detect small changes in axon terminals than the use of vibratome sections. The results of this study are consistent with previous findings by our group in 6 and 14 month old Thy1-aSyn mice (Watson et al. 2012). Microglial activation and the upregulation of TNF-α mRNA and protein levels were not observed in the substantia nigra of 1 month old Thy1-aSyn mice as seen in these mice at 6 and 14 months of age. Together, these results suggest that specific microglial activation associated with the TNF-α cytokine network begins in the striatum of Thy1-aSyn mice, and it progressively intensifies and spreads into the substantia nigra over time. It is notable that this microglial activation occurs in the phases of development when there is no dopaminergic cell death observed in these mice, suggesting that activation is not due to toxic factors released by dying neurons but possibly due to the direct action of alpha-synuclein on microglial cells.

Our findings are comparable to a recent study by Su and colleagues that demonstrated that overexpression of mutant alpha-synuclein induced prominent microglial-mediated inflammation in the substantia nigra and striatum (Su et al. 2009). This study reported that inflammation proceeded at 1 month of age, but was resolved by 6 months of age due to the toxic effects of the mutant alpha-synuclein expression. However, this study examined mutant overexpression, which is inherently more toxic than the wildtype alpha-synuclein used here. Previous studies from our lab, however, show microglial activation persisting at 6 months of age, supporting the idea that Thy1-aSyn mice display a more protracted and physiologically relevant phenotype. Furthermore, Thy1-aSyn mice displayed motor deficits that became progressively worse with age. Behavioral studies revealed that Thy1-aSyn mice performed worse in motor performance and coordination on the challenging beam test at 6-8 months of age compared with these mice at 2 and 4 months of age (Fleming et al. 2004). Again, these data propose that progressive microglial activation with age may play a causative role in the enhancement of motor deficits seen in Thy1-aSyn mice.

It is notable that there is regionally specific microglial activation in the striatum in Thy1-aSyn mice at 1 month of age. Interestingly, such patterns of inflammation are not found in the cortex despite that the expression of alpha-synuclein is widespread in these mice (Rockenstein et al. 2002). In addition, microglial activation is localized to the striatal region of the brain early in development, which in Thy1-aSyn mice do not contain large aggregates of alpha-synuclein. Conversely, areas that do contain alpha-synuclein inclusions, such as the olfactory bulb, substantia nigra and locus coeruleus, do not display signs of early microglial activation or associated inflammatory changes (Chesselet et al. 2012, data not shown). Therefore, these data

suggest that the striatum and its residing microglia are more susceptible to the effects of alpha-synuclein overexpression or that there is a different species of alpha-synuclein present in this region of the brain. It can also be hypothesized that alpha-synuclein is acting synergistically with other factors in the striatum to induce localized microglial activation. A recent study at UCLA showed increased observed increased extracellular dopamine in the striatum of Thy1-aSyn mice (Lam et al. 2011). Dopamine may cause striatal microglia to be primed, in which the altered microglia can become hypersensitive in response to alpha-synuclein and as a result increase their inflammatory activities. Comparing patterns of microglial activation in mouse models that are characterized with increased extracellular dopamine in the striatum to those observed in Thy1-aSyn mice may provide a better understanding of the factors that cause localized inflammatory alterations in Thy1-aSyn mice.

The results of prior studies from our group have indicated the microglia activated in the substantia nigra differ phenotypically from the microglia activated in the striatum of Thy1-aSyn mice. At 1 month of age, there was a significant increase in activated Iba-1^{+} microglia only in the striatum, with no significant changes in CD11b mRNA expression in both the striatum and substantia nigra. As the Thy1-aSyn mice aged to 6 months of age, our group found that there is increased activation of Iba-1^{+} microglia in both the striatum and substantia nigra along with increased levels of CD11b mRNA (Watson et al. 2012; accepted). CD11b is a cell surface marker that is constitutively expressed on microglia, but can be upregulated under certain conditions (Frank et al. 2006). Iba-1 is a microglia-specific calcium-binding protein involved in microglial proliferation, migration, phagocytosis and the production of bioactive agents (Imai et al. 2002). More unpublished work by our group concluded that CD68 expression on microglial

cells in the substantia nigra of Thy1-aSyn mice were not altered compared to WT, where CD68 is a marker for phagocytotic cells. Together, these results suggest that microglia found in the substantia nigra are not involved in phagocytosis or other macrophagic phenotypes, but instead linked to cytokine production and antigen presentation. Therefore, the expression of different markers on the microglial cells in the substantia nigra and the striatum offers the possibility that there may be different mechanisms leading to microglial activation in these two regions in Thy1-aSyn mice.

In this study, microglial activation in the striatum was determined to be exclusively associated with increased levels of TNF-α mRNA in Thy1-aSyn mice at 1 month of age. TNF-α synthesis progressively intensified in both the substantia nigra and striatum of these mice with age, where both TNF-α mRNA and protein levels were significantly increased in Thy1-aSyn mice compared to WT (Watson et al. 2012; accepted). Given that different microglial phenotypes in separate regions of the brain were both involved in TNF-α signaling and that TNF-α was the only pro-inflammatory cytokine that exhibited upregulation, we can deduce that TNF-α may be the key transducer of alpha-synuclein toxicity. Pro-inflammatory cytokine production in the central nervous system has been linked to cell death and neurodegenerative disease, where studies have drawn attention to the role of TNF-α in the pathogenesis of PD (Hartmann et al. 2002, Sriram et al. 2002). Clincally, genetic polymorphisms in the TNF-α gene have been noted in PD patients (Bialecka et al. 2008). Interestingly, the accumulation of wildtype and mutant species of alpha-synuclein are documented to induce TNF-α secretion by microglial cells and even increase TNF-α mediated cell death (Stefanova et al. 2003, Su et al. 2008, Klegeris et al. 2008). Future experimentation that evaluates the signaling molecules downstream from TNF-α including

stress-activated protein kinases, such as c-Jun-N-terminal-kinase (JNK) and p38, NK-κB or caspase-8 (Li et al. 2008) and their association with alpha-synuclein-induced microglial activation would shed light on the effects of TNF-α in the pathogenesis of PD. It would also prove worthwhile to understand the relationship between selective microglial secretion of TNF-α and the neuronal cell death characterized in PD. In summary, the results presented in this thesis propose that widespread alpha-synuclein overexpression resulted in phenotypically distinct microglial activation beginning in the striatum, suggesting that alpha-synuclein overexpression capable of activating early inflammatory events that are associated with PD pathology.

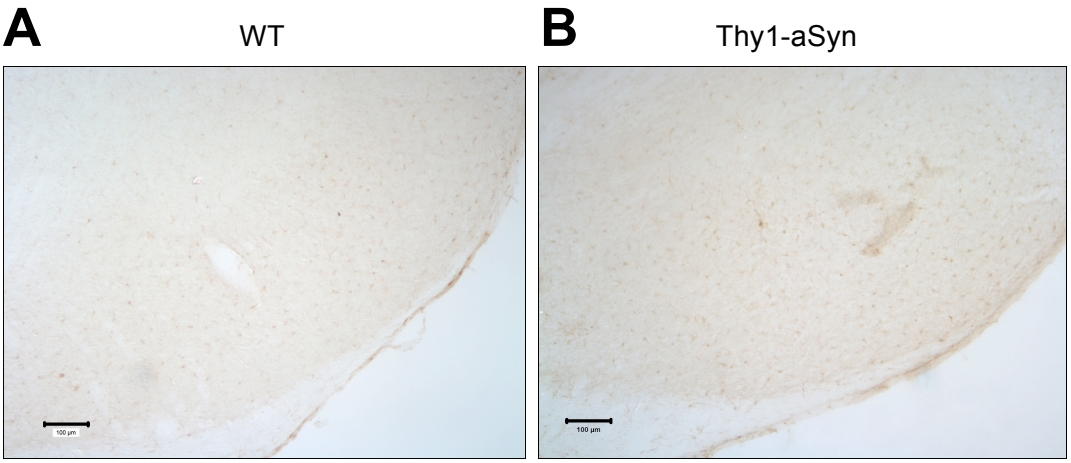

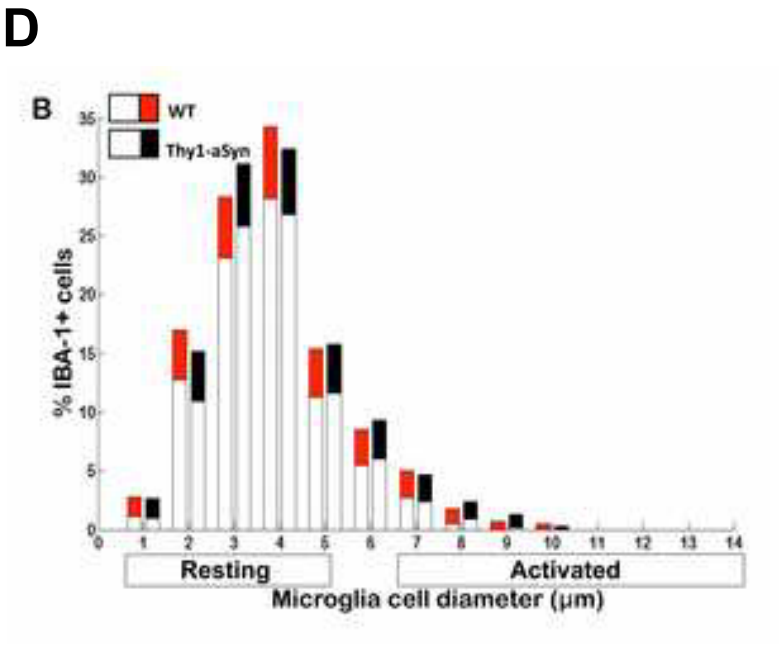

Figure 1. Microglial activation in the substantia nigra of WT and Thy1-aSyn mice. The diameters of Iba-1 positive cells (Iba-1$^+$) were measured in arbitrarily picked sections of the substantia nigra of 1 month old wild-type and Thy1-aSyn mice. **(A)** Representative image of Iba-1$^+$ immunohistochemistry in the substantia nigra of 1 month old WT mice. 10x magnification, scale bar = 100 μm. **(B)** Representative images of Iba-1$^+$ immunohistochemistry in the substantia nigra of 1 month old Thy1-aSyn mice. 10x magnification, scale bar = 100 μm. **(D)** Bootstrapping analysis revealed no significant differences in Iba-1$^+$ microglia counts in the substantia nigra between groups. Data are expressed in 95% confidence intervals of mean percentages of Iba-1$^+$ microglia count. n = 4 mice per group.

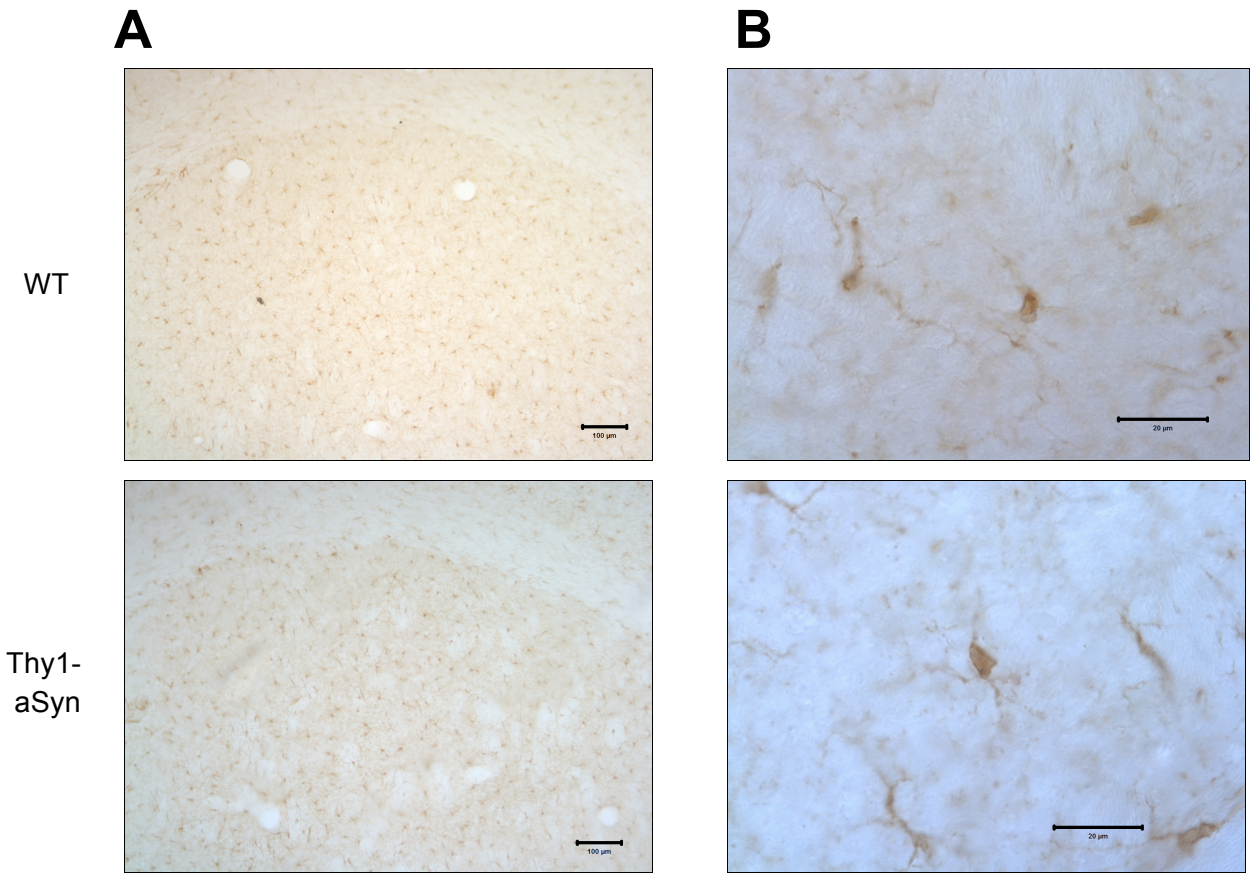
A
B
WT
Thy1-aSyn
100 µm
20 µm

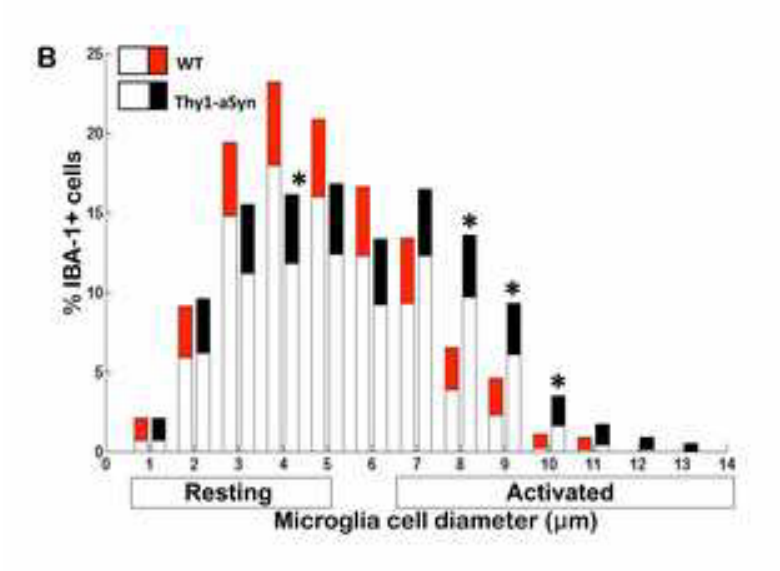
C
B
WT
Thy1-aSyn
% IBA-1+ cells
Resting
Activated
Microglia cell diameter (µm)

Figure 2. Microglial activation in the striatum of WT and Thy1-aSyn mice. The diameters of Iba-1 positive cells (Iba-1^+) were measured in arbitrarily picked sections of the striatum of 1 month old wild-type and Thy1-aSyn mice. **(A)** Representative images of Iba-1^+ immunohistochemistry in the striatum of 1 month old WT and Thy1-aSyn mice at 10x magnification. Scale bar = 100 μm. **(B)** Representative images of Iba-1^+ immunohistochemistry in the striatum of 1 month old WT and Thy1-aSyn mice at 100x magnification. Scale bar = 20 μm. **(C)** Bootstrapping analysis revealed statistically significant differences in activated amoeboid Iba-1^+ microglia in the striatum. Data are expressed in 95% confidence intervals of mean percentages of Iba-1^+ microglia count. *$p < 0.05$ compared to WT. n = 3 mice per group.

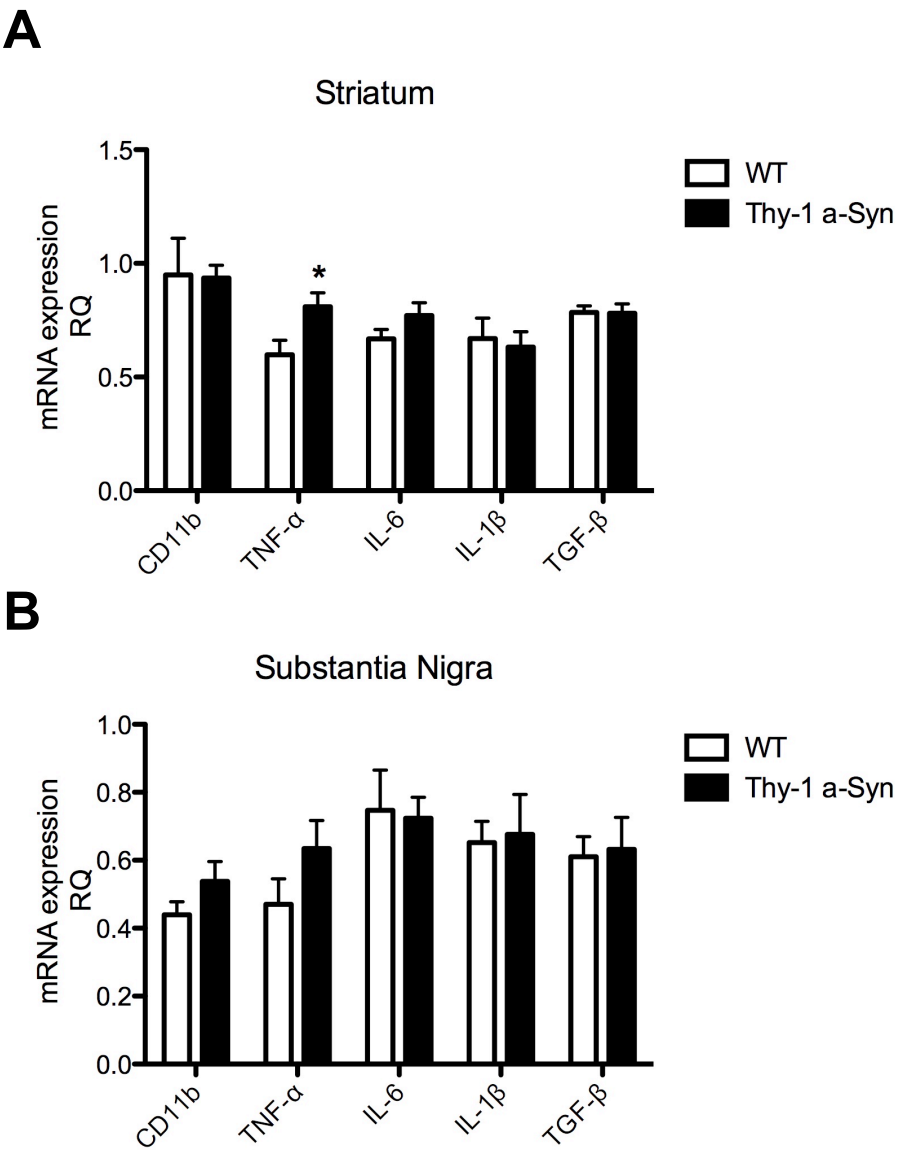

Figure 3. Assessment of microglial activation and cytokine gene expression in the striatum and substantia nigra of WT and Thy1-aSyn mice. mRNA expression of CD11b (constitutively expressed by microglia), pro-inflammatory cytokines (TNF-α, IL-6, IL-1β), and anti-inflammatory cytokine TGF-β in the striatum and substantia nigra of 1 month old WT and Thy1-aSyn mice were assessed by quantitative RT-PCR using Taqman chemistry. **(A)** Student's t-test revealed that TNF-α mRNA expression was significantly increased in the striatum of Thy1-aSyn mice compared to WT. *$p < 0.05$, $n = 7$ mice per group. **(B)** Student's t-test revealed no significant differences in microglial and cytokine mRNA expressions in the substantial nigra between WT and Thy1-aSyn mice. $n = 6$-7 mice per group. All data are expressed as relative quantification (RQ) and are mean ± SEM. Gene expressions were normalized using the geometric means of the relative concentration of the housekeeping genes β-actin, HPRT and ATP5B.

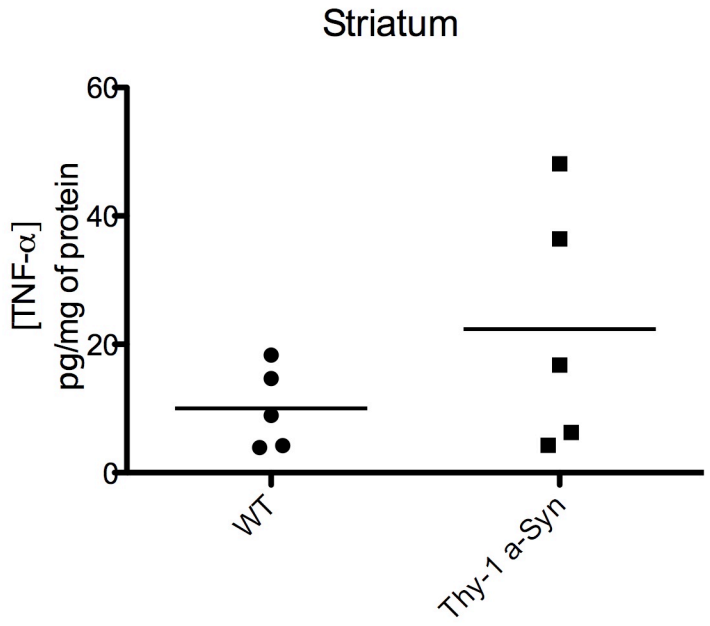

Figure 4. TNF-α concentration in the striatum of Thy1-aSyn mice. The protein concentration of TNF-α was assessed by ELISA in the striatum of 1 month old WT and Thy1-aSyn mice. Student's t-test revealed no significant differences between groups. Data are expressed as pg of TNF-α per mg of protein. n = 5 mice per group.

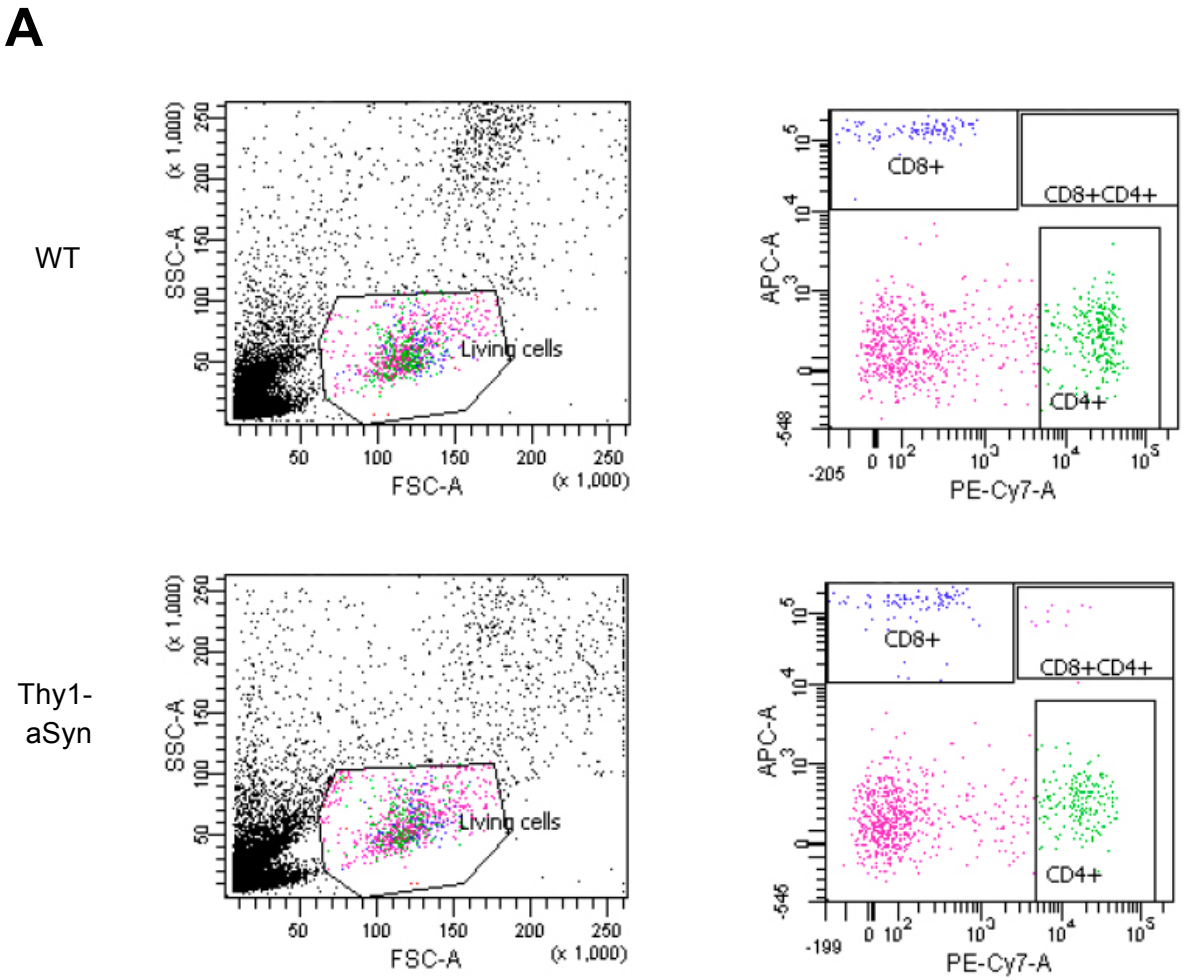
A
WT
Thy1-aSyn
SSC-A
(x 1,000)
FSC-A
(x 1,000)
Living cells
CD8+
CD8+CD4+
CD4+
APC-A
PE-Cy7-A
-548
-205
-546
-199

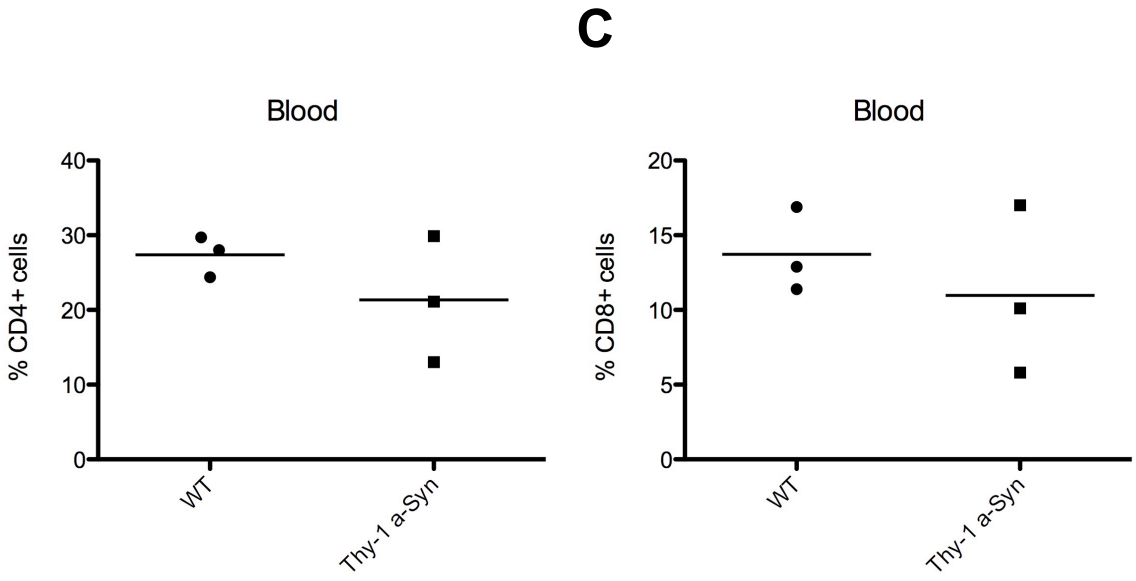
B
Blood
% CD4+ cells
WT
Thy-1 a-Syn
C
Blood
% CD8+ cells
WT
Thy-1 a-Syn

Figure 5. Detection of $CD4^+$ and $CD8^+$ T cells in the blood of WT and Thy1-aSyn mice. $CD4^+$ and $CD8^+$ T cells were measured in the blood of 1 month old wild-type and Thy1-aSyn mice using flow cytometry. **(A)** Representative dot plots of flow cytometry results assessed the percentage of $CD4^+$ and $CD8^+$ T cells in the blood of 1 month old WT and Thy1-aSyn mice. Following data acquisition, living cells were gated on $CD4^+$ events for helper T cells and $CD8^+$ events for cytotoxic T cells. **(B)** Non-parametric Mann-Whitney test revealed no significant difference in $CD4^+$ T cell percentages between groups. Data are raw percentages of $CD4^+$ cell counts in the blood. n = 3 mice per group. **(C)** Non-parametric Mann-Whitney test revealed no significant difference in $CD8^+$ T cell percentages between groups. Data are raw percentages of $CD8^+$ cell counts in the blood. n = 3 mice per group.

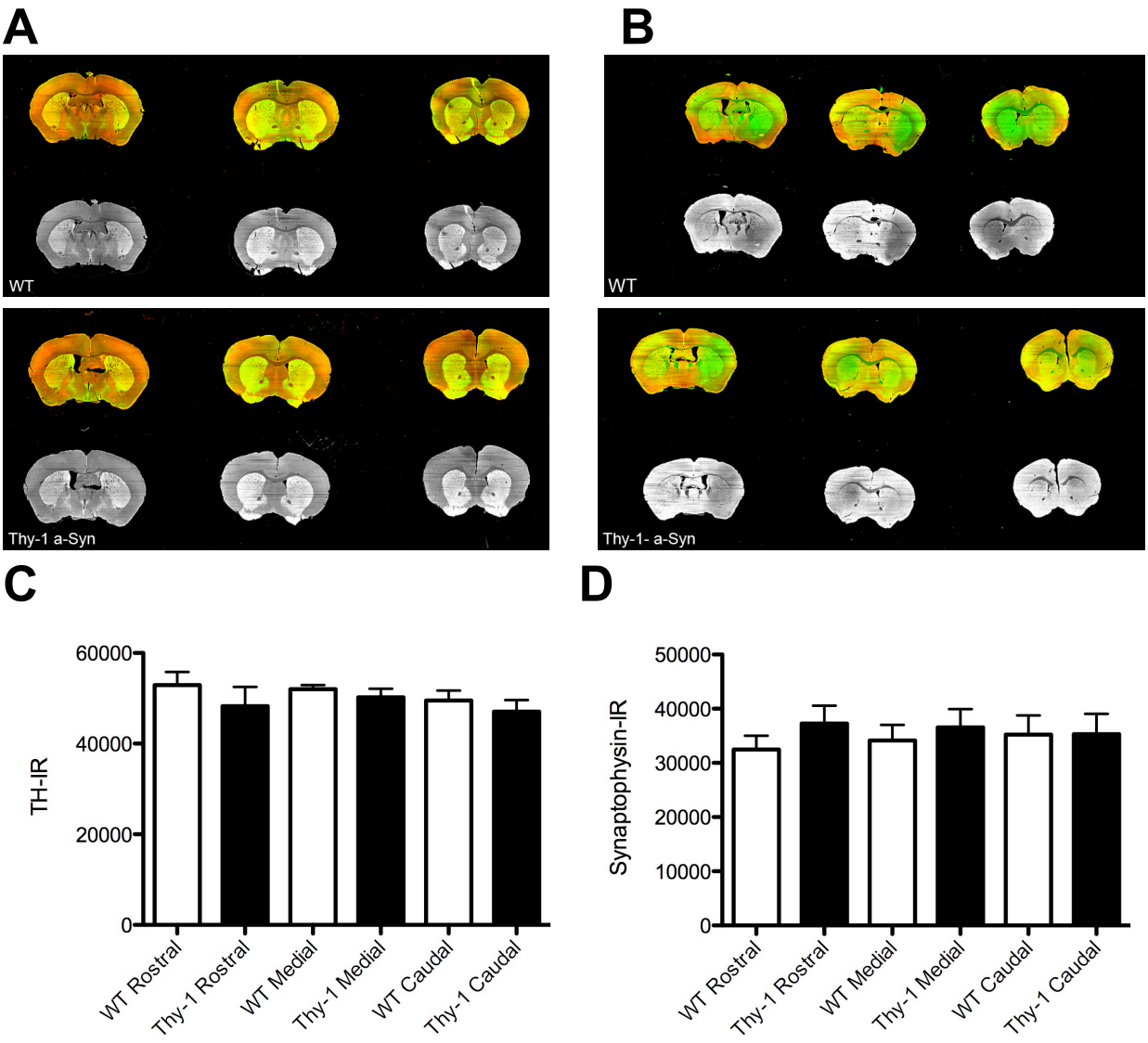

Figure 6. Tyrosine hydroxylase (TH) and synaptophysin expression in the striatum of WT and Thy1-aSyn mice. TH and synaptophysin immunofluorescence were measured in the striatum of 1 month old WT and Thy1-aSyn mice. Striatal sections were stained with anti-TH and anti-synaptophysin, followed by Cy3 and Cy5 secondary antibody, respectively, for immunofluorescence. **(A)** Representative images of TH immunofluorescence in the striatum of 1 month old WT (top) and Thy1-aSyn (bottom) mice. **(B)** Representative images of synaptophysin immunofluorescence in the striatum of 1 month old WT (top) and Thy1-aSyn (bottom) mice visualized. **(C)** No significant differences in TH expression were found in arbitrarily selected rostral, medial and caudal sections of the striatum between groups. Data are mean ± SEM. n = 6 mice per group. **(D)** No significant differences in TH expression were found in arbitrarily selected rostral, medial and caudal sections of the striatum between groups. Data are mean ± SEM. n = 6 mice per group. Immunofluorescence levels in the striatum were analyzed by one-way ANOVA, post-hoc Fisher's LSD.

References

Banati RB, Daniel SE, Blunt SB (1998). Glial pathology but absence of apoptotic nigral neurons in long-standing Parkinson's disease. Movement Disorders 13(2): 221-227.

Batchelor PE, Liberatore GT, Wong JY, Porritt MJ, Frerichs F, Donnan GA, Howells DW (1999). Activated macrophages and microglia induce dopaminergic sprouting in the injured striatum express brain-derived neurotrophic factor and glial cell line-derived neurotrophic factor. Jounral of Neuroscience 19(5): 1708-1716.

Bekris ML, Mata IF, Zabetian CP (2010). The genetics of Parkinson disease. Journal of Geriatric Psychiatry and Neurology 23(4): 228-242.

Bialecka M, Klodowska-Duda G, Kurzawski M, Slawek J, Gorzkowska A, Opala G, Bialecki P, Sagan L, Drozdzik M (2008). Interleukin-10 (IL10) and tumor necrosis factor alpha (TNF) gene polymorphisms in Parkinson's disease patients. Parkinsonism Related Disorders 14(8): 636-640.

Braak H, Del Tredici K, Rub U, de Vos RA, Jansen Steur EN, Braak E (2003). Staging of brain pathology related to sporadic Parkinson's disease. Neurobiology of Aging 24(2): 197-211. Djaldetti R, Lev N, Melamed E (2009). Lesions outside the CNS in Parkinson's disease. Movement Disorders 24(6): 793-800.

Braak H, Ghebremedhin E, Rub U, Bratzke H, Del Tredici K (2004). Stages in the development of Parkinson's disease-related pathology. Cells and Tissue Research 318(1): 121-134.

Brochard V, Combadiere B, Prigent A, Laouar Y, Perrin A, Beray-Berthat V, Bonduelle O, Alvarez-Fischer D, Callebert J, Launay JM, Duyckaerts C, Flavell RA, Hirsch EC, Hunot S (2009). Infiltration of CD4+ lymphocytes into the brain contributes to neurodegeneration in a mouse model of Parkinson disease. Journal of Clinical Investigation 119(1): 182-192.

Chaudhuri KR, Healy DG, Schapira AH (2006). Non-motor symptoms of Parkinson's disease: diagnosis and management. The Lancet Neurology 5(3): 235-245.

Chaudhuri KR, Schapira AH (2009). Non-motor symptoms of Parkinson's disease: dopaminergic pathophysiology and treatment. The Lancet Neurology 8(5): 464-474.

Chesselet MF, Richter F (2011). Modelling of Parkinson's disease in mice. The Lancet Neurology 10(12): 1108-1118.

Chesselet MF, Richter F, Zhu C, Magen I, Watson MB, Subramaniam SR (2012). A progressive

mouse model of Parkinson's disease: the Thy1-aSyn ("Line 61") mice. Neurotherapeutics 9(2): 297-314.

Clayton DF, George JM (1999). Synucleins in synaptic plasticity and neurodegenerative disorders. Journal of Neuroscience Research 58(1):120-129.

Croisier E, Moran LB, Dexter DT, Pearce RK, Graeber MB (2005). Microglial inflammation in the parkinsonian substantia nigra: relationship to alpha-synuclein deposition. Journal of Neuroinflammation 2:14.

Czlonkowska A, Kohutnicka M, Kurkowska-Jastrzebska I, Czlonkowska A (1996). Microglial reaction in MPTP (1-methyl-4-phenyl-1,2,3,6-tetrahydropyridine) induced Parkinson's disease mice model. Neurodegeneration 5(2): 137-143.

Davidson WS, Jonas W, Clayton DF, George JM (1998). Stabilization of alpha-synuclein secondary structure upon binding to synthetic membranes. Journal of Biological Chemistry 273(16): 9443-9449.

Davie CA (2008). A review of Parkinson's disease. British Medical Bulletin 86: 109-127.

Fleming SM, Salcedo J, Fernagut PO, Rockenstein E, Masliah E, Levine MS, Chesselet MF (2004). Early and progressive sensorimotor anomalies in mice overexpressing wild-type human alpha-synuclein. Journal of Neuroscience 24(42): 9434-9440.
Fernagut PO, Hutson CB, Fleming SM, Tetreaut NA, Salcedo J, Masliah E, Chesselet MF (2007). Behavioral and histopathological consequences of paraquat intoxication in mice: effects of alpha-synuclein over-expression. Synapse 61(12): 991-1001.

Fleming SM, Tetreault NA, Mulligan CK, Hutson CB, Masliah E, & Chesselet MF (2008). Olfactory deficits in mice overexpressing human wildtype alpha-synuclein. European Journal of Neuroscience 28(2): 247-256.

Francis JW, Von Visger J, Markelonis GJ, Oh TH (1995). Neuroglial responses to the dopaminergic neurotoxicant 1-methyl-4-phenyl-1,2,3,6-tetrahydropyridine in mouse striatum. Neurotoxicology and Teratology 17(1): 7-12.

Frank MG, Wieseler-Frank JL, Watkins LR, Maier SF (2006). Rapid isolation of highly enriched and quiescent microglia from adult rat hippocampus: immunophenotypic and functional characteristics. Journal of Neuroscience Methods 151(2): 121-130.

Gao HM, Kotzbauer PT, Uryu K, Leight S, Trojanowski JQ, Lee VM (2008). Neuroinflammation and oxidation/nitration of α-synuclein linked to dopaminergic neurodegeneration. Journal of Neuroscience 28(30): 7687-7698.

Gao HM, Hong JS (2011). Gene-environment interactions: key to unraveling the mystery of Parkinson's disease. Progress in Neurobiology 94(1):1-19.

Hartmann A, Mouatt-Prigent A, Faucheux BA, Agid Y, Hirsch EC (2002). FADD: A link between TNF family receptors and caspases in Parkinson's disease. Neurology 58(2): 308-310.

Hirsch EC, Breidert T, Rousselet E, Hunot S, Hartmann A, Michel PP (2003). The role of glial reaction and inflammation in Parkinson's disease. Annals of the New York Academy of Sciences 991:214-228.

Horowitz MP, & Greenamyre JT. (2010). Gene-Environment Interactions in Parkinson's disease: the importance of animal modeling. Clinical Pharmacology and Therapeutics 88(4): 467-474.

Hunot S, Hirsch EC (2003). Neuroinflammatory processes in Parkinson's disease. Annals of Neurology 53 Suppl 3:S49-58; discussion S58-60.

Ibanez P, Bonnet AM, Debarges B, Lohmann E, Tison F, Pollak P, Agid Y, Durr A, Brice A (2004). Causal relation between alpha-synuclein gene duplication and familial Parkinson's disease. Lancet 364(9440): 1169-1171.

Imai Y, Ibata I, Ito D, Ohsawa K, Kohsaka S (1996). A novel gene iba1 in the major histocompatibility complex class III region encoding an EF hand protein expressed in a monocytic lineage. Biochemical and Biophysical Research Communications 224(3): 855-862.

Imamura K, Hishikawa N, Sawada M, Nagatsu T, Yoshida M, Hashizume Y (2003). Distribution of major histocompatibility complex class II-positive microglia and cytokine profile of Parkinson's disease brains. Acta Neuropathologica 106(6):518-526.

Jankovic J (2008). Parkinson's disease: clinical features and diagnosis. Journal of Neurology, Neurosurgery, and Psychiatry 79: 368-376.

Kim YS, Joh TH (2006). Microglia, major player in the brain inflammation: their roles in the pathogenesis of Parkinson's disease. Experimental and Molecular Medicine 38(4): 333-347.

Klegeris A, Glasson BI, Zhang H, Maguire J, Pelech S, McGeer PL (2006). Alpha-synuclein and its disease-causing mutants induce ICAM-1 and IL-6 in human astrocytes and astrocytoma cells.

Klegeris A, Pelech S, Glasson BI, Maguire J, Zhang H, McGeer EG, McGeer PL (2008). Alpha-synuclein activates stress signaling protein kinases in THP-1 cells and microglia. Neurobiology of Aging 29(5): 739-752.

Kreutzberg GW (1996). Microglia: a sensor for pathological events in the CNS. Trends in Neurosciences 19(8): 312-318.

Kruger R, Kuhn W, Muller T, Woitalla D, Graeber M, Kosel S, Przuntek H, Epplen JT, Schols L, Riess O (1998). Ala30Pro mutation in the gene encoding alpha-synuclein in Parkinson's disease. Nature Genetics 18(2): 106-108.

Lam HA, Wu N, Cely I, Kelly RL, Hean S, Richter F, Magen I, Cepeda C, Ackerson LC, Walwyn W, Masliah E, Chesselet MF, Levine MS, Maidment NT (2011). Elevated tonic extracelluar dopamine concentration and altered dopamine modulation of synaptic activity precede dopamine loss in the striatum of mice overexpressing human α-synuclein. Journal of Neuroscience Research 89(7): 1091-1102.

Lee EJ, Woo MS, Moon PG, Baek MC, Choi IY, Kim WK, Junn E, Kim HS (2010). α-Synuclein activates microglia by inducing the expression of matrix metalloproteinases and the subsequent activation of protease-activated receptor-1. Journal of Immunology 185(1): 615-623.

Lew M (2007). Overview of Parkinson's disease. Pharmacotherapy 27(12): 155S-160S.

Li H, Lin X (2008). Positive and negative signaling components involved in TNFalpha-induced NF-kappaB activation. Cytokine 41(1): 1-8.

Lykkebo S, Jensen PH (2002). Alpha-synuclein and presynaptic function: implications for Parkinson's disease. Neuromolecular Medicine 2(2): 115-129.

Maroteaux L, Scheller RH (1991). The rat brain synucleins; family of proteins transiently associated with neuronal membrane. Molecular Brain Research 11(3-4): 335-343.

McGeer PL, Itagaki S, Boyes BE, McGeer EG (1988). Reactive microglia are positive for HLA-DR in the substantia nigra of Parkinson's and Alzheimer's disease brains. Neurology 38(8): 1285-1291.

Nagatsu T, Mogi M, Ichinose H, Togari A (2000). Cytokines in Parkinson's disease. Journal of Neural Transmission Supplementum (58): 143-51.

Nagatsu T, Sawada M (2005). Inflammatory process in Parkinson's disease: role for cytokines. Current Pharmacological Design 11(8): 999-1016.

National Institute of Neurological Diseases and Stroke, National Institute of Health; http://www.ninds.nih.gov/

Polymeropoulos MH, Lavedan C, Leroy E, Ide SE, Dehejia A, Dutra A, Pike B, Root H, Rubenstein J, Boyer R, Stenroos ES, Chandrasekharappa S, Athanassiadou A, Papapetropoulos T, Johnson WG, Lazzarini AM, Duvoisin RC, Di Iorio G, Golbe LI, Nussbaum RL (1997). Mutation in the alpha-synuclein gene identified in families with Parkinson's disease. Science 276(5321): 2045-2047.

Rapplold PM, Lynd-Balta E, Joseph SA (2006). P2X7 receptor immunoreactive profile confined to resting and activated microglia in the epileptic brain. Brain Research 1089(1): 171-178.

Reynolds AD, Glanzer JG, Kadiu I, Ricardo-Dukelow M, Chaudhuri A, Ciborowski P, Cerny R, Gelman B, Thomas MP, Mosley RL, Gendelman HE (2008). Nitrated alpha-synuclein-activated microglial profiling for Parkinson's disease. Jounral of Neurochemistry 104(6): 1504-1525.

Rockenstein E, Mallory M, Hashimoto M, Song D, Shults CW, Lang I, Masliah E (2002). Differential neuropathological alterations in transgenic mice expressing alpha-synuclein from the platelet-derived growth factor and Thy-1 promoters. Journal of Neuroscience Research 68(5): 568-578.

Ross CA, Smith WW (2007). Gene-environment interactions in Parkinson's disease. Parkinsonism and Related Disorders 13 Suppl 3: S309-315.

Sanchez-Guajardo V, Febbraro F, Kirik D, Romero-Ramos M (2010). Microglia acquire distinct activation profiles depending on the degree of alpha-synuclein neuropathology in a rAAV based model of Parkinson's disease. PLoS One 5(1): e8784.

Sapir S, Ramig L, Fox C (2008). Speech and swallowing disorders in Parkinson disease. Current Opinions in Otolaryngology & Head and Neck Surgery 16(3): 205-210.

Shapiro LA, Perez ZD, Foresti ML, Arisi GM, Ribak CE (2009). Morphological and ultrastructural features of Iba1-immunolabeled microglial cells in the hippocampal dentate gyrus. Brain Research 1266:29-36.

Singleton AB, Farrer M, Johnson J, Singleton A, Hague S, Kachergus J, Hulihan M, Peuralinna T, Dutra A, Nussbaum R, Lincoln S, Crawley A, Hanson M, Maraganore D, Adler C, Cookson

MR, Muenter M, Baptista M, Miller D, Blancato J, Hardy J, Gwinn-Hardy K (2003). alpha-Synuclein locus triplication causes Parkinson's disease. Science 302(5646): 841.

Sriram K, Matheson JM, Benkovic SA, Miller DB, Luster MI, O'Callaghan JP (2002). Mice deficient in TNF receptors are protected against dopaminergic neurotoxicity: implications in Parkinson's disease. FASEB 16(11): 1474-1476.

Stefanis L (2012). α-Synuclein in Parkinson's disease. Cold Spring Harbor Perspectives in Medicine 2(2):a009399.

Stefanova N, Schanda K, Klimaschewski L, Poewe W, Wenning GK, Reindl M (2003). Tumor necrosis factor-alpha-induced cell death in U373 cells overexpressing alpha-synuclein. Journal of Neuroscience Research 73(3): 334-340.

Su X, Maguire-Zeiss KA, Giuliano R, Prifti L, Venkatesh K, Federoff HJ (2008). Synuclein activates microglia in a model of Parkinson's disease. Neurobiology of Aging 29(11): 1690-1701.

Su X, Federoff GH, Maguire-Zeiss KA (2009). Mutant alpha-synuclein overexpression mediates early proinflammatory activity. Neurotoxicity Research 16(3): 238-254.

Surmeier DJ, Ding J, Day M, Wang Z, Shen W (2007). D1 and D2 dopamine-receptor modulation of striatal glutamatergic signaling in striatal medium spiny neurons. Trends in Neurosciences 30(5): 228-235.

Watson JB, Hatami A, David H, Masliah E, Roberts K, Evans CE, Levine MS (2009). Alterations in corticostriatal synaptic plasticity in mice overexpressing human α-synuclein. Neuroscience 159(2): 501-513.

Watson MB, Richter F, Lee SK, Gabby L, Wu J, Masliah E, Effros RB, Chesselet MF (2012). Regionally-specific microglial activation in young mice over-expressing human wildtype alpha-synuclein. Experimental Neurology, in press.

Zhang W, Wang T, Pei Z, Miller DS, Wu X, Block ML, Wilson B, Zhang W, Zhou Y, Hong JS, Zhang J (2005). Aggregated alpha-synuclein activates microglia: a process leading to disease progression in Parkinson's disease. FASEB Journal 19(6): 533-542.

Zhang W, Dallas S, Zhang D, Guo JP, Pang H, Wilson B, Miller DS, Chen B, Zhang W, McGeer PL, Hong JS, Zhang J (2007). Microglial PHOX and Mac-1 are essential to the enhanced dopaminergic neurodegeneration elicited by A30P and A53T mutant alpha-synuclein. Glia

55(11): 1178-1188.

Ziemssen T, Reichmann H (2007). Non-motor dysfunction in Parkinson's disease. Parkinsonism & Related Disorders 13(6): 323-332.